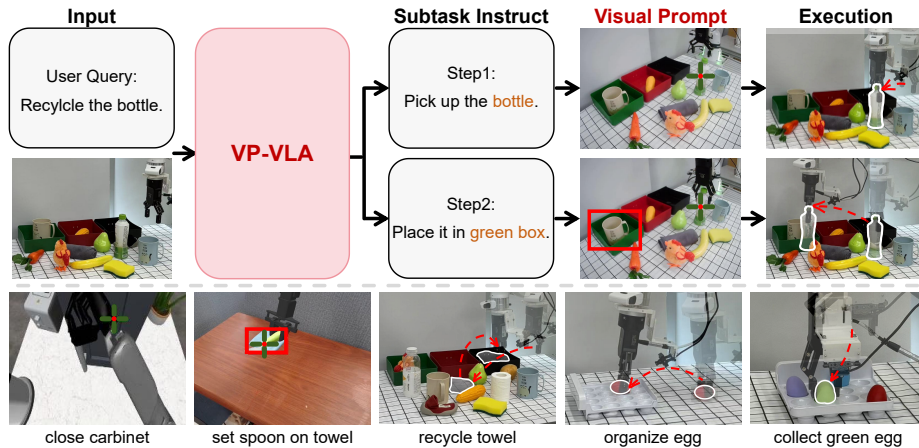


# VP-VLA: Visual Prompting as an Interface for Vision-Language-Action Models

Zixuan Wang<sup>\*,1</sup>, Yuxin Chen<sup>\*,1</sup>, Yuqi Liu<sup>\*,2</sup>, Jinhui Ye<sup>1</sup>, Pengguang Chen<sup>3</sup>,  
Changsheng Lu<sup>1</sup>, Shu Liu<sup>3</sup>, and Jiaya Jia<sup>1,3</sup>

<sup>1</sup> HKUST    <sup>2</sup> CUHK    <sup>3</sup> SmartMore



**Fig. 1:** VP-VLA leverages a dual-system architecture to bridge high-level reasoning and low-level control, maintaining competitive performance across a wide variety of tasks on in-distribution and out-of-distribution settings.

**Abstract.** Vision-Language-Action (VLA) models typically map visual observations and linguistic instructions directly to robotic control signals. This “black-box” mapping forces a single forward pass to simultaneously handle instruction interpretation, spatial grounding, and low-level control, often leading to poor spatial precision and limited robustness in out-of-distribution scenarios. To address these limitations, we propose VP-VLA, a dual-system framework that decouples high-level reasoning and low-level execution via a structured visual prompting interface. Specifically, a “System 2 Planner” decomposes complex instructions into sub-tasks and identifies relevant target objects and goal locations. These spatial anchors are then overlaid directly onto visual observations as structured visual prompts, such as crosshairs and bounding boxes. Guided by these prompts and enhanced by a novel auxiliary visual grounding objective during training, a “System 1 Controller” reliably generates precise low-level execution motions. Experiments on the Robocasa-GR1-Tabletop benchmark and SimplerEnv simulation demonstrate that VP-VLA improves success rates by 5% and 8.3%, surpassing competitive baselines including QwenOFT and GR00T-N1.6.

\* Equal contribution.

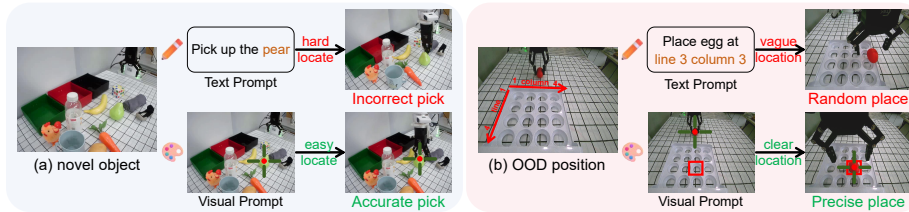


**Fig. 2:** Existing VLA models often fail to achieve precise localization (Red), whereas our VP-VLA leverages visual prompts to ensure accurate target placement (Green) across novel objects and unseen spatial configurations.

**Keywords:** Vision-and-Language Models · Manipulation · Visual-Language-Action Models

## 1 Introduction

Recent advances in vision language models (VLMs) have revolutionized robotic manipulation. Vision-language-action (VLA) models, in particular, aim to bridge semantic understanding and low-level control by fine-tuning pretrained VLMs on large-scale robotic datasets. By doing so, these models inherit strong real-world priors while acquiring embodied skills, offering a promising path toward generalist manipulation policies [2, 3, 27].

Despite these successes, existing VLA frameworks often overfit to specific training scene distributions rather than truly grounding instructions in the environment. This is evidenced by recent findings [10, 48] showing that substituting meaningful language with gibberish barely affects performance. Consequently, these policies often fail when encountering novel object categories or unseen spatial positions, as illustrated in Fig. 2. To mitigate these issues, several approaches introduce intermediate interfaces, such as goal images [44] or dense geometric supervision [43, 47], to provide fine-grained guidance. However, these methods typically focus on static, single-task scenarios and rely on rigid interface representations. They often fail to account for the dynamic nature of multi-stage tasks, where the required visual focus and affordance should evolve as the task progresses. Furthermore, curating dense geometric data for these models is prohibitively expensive, and the quality of predicted affordances remains inconsistent. More critically, current VLA systems struggle to effectively integrate high-level reasoning [14] with low-level execution within end-to-end models [33].

To address these challenges, we propose VP-VLA, a decoupled dual-system VLA framework. VP-VLA utilizes visual prompts as an explicit, structured interface between high-level reasoning (the “System 2 Planner”) and low-level execution (the “System 1 Controller”). Unlike end-to-end models that attempt to implicitly solve instruction interpretation, spatial relation inference, and execution simultaneously, our approach employs a pretrained VLM as a high-level planner. This planner decomposes complex instructions into sub-tasks and iden-

tifies relevant target objects and goal locations. These spatial references are then translated into structured visual prompts, including crosshair markers for targets and bounding boxes for placement regions, which are overlaid onto the visual observations for the low-level controller. By integrating visual prompts directly in the image space, we transform complex linguistic instructions into precise spatial anchors. To ensure the policy effectively utilizes these cues, we introduce an auxiliary grounding objective. This objective encourages explicit spatial awareness within the VLA controller during training.

We evaluate VP-VLA on diverse simulation benchmarks and real-world scenarios, where it consistently outperforms state-of-the-art methods: On Robocasa-GR1-Tabletop benchmark, VP-VLA improves the average success rate by 5% over the baseline, surpassing competitive models like GR00T-N1.6 [2] without requiring additional large-scale robotic pretraining. On SimplerEnv benchmark, our method achieves substantial absolute improvement of +8.3% over baseline, surpassing prior VLA models including  $\pi_{0.5}$  [12]; In real-world cluttered scenario, our method consistently yield superior performance on both in-distribution and out-of-distribution evaluations. Our contributions are summarized as follows:

- We propose VP-VLA, a novel framework that decouples high-level reasoning from low-level control through a structured visual prompting interface.
- We introduce a visual grounding objective during training that enhances the spatial precision and robustness of VLA models.
- Experiments on Robocasa-GR1-Tabletop, SimplerEnv and real-world scenario demonstrate VP-VLA achieves consistent gains over strong baselines.

## 2 Related Work

**Vision-Language-Action Models.** Vision-language-action (VLA) models have become a practical paradigm for general-purpose robotic manipulation, translating open-ended semantic instructions into visuomotor policies [3, 18, 40]. Leveraging large-scale robot demonstration datasets [4, 5, 13, 16, 25, 30, 39], recent VLAs generalize across diverse tasks and objects by integrating large-scale vision-language models [11, 29, 37, 38], multi-modal inputs, and heterogeneous data sources, including real-robot trajectories, human videos, and synthetic simulations. However, most methods adopt a monolithic architecture that tightly couples reasoning, spatial grounding, and action generation, hindering task decomposition and intermediate representation [3, 18, 45]. Under distribution shifts or personalized scenarios [19], VLAs remain brittle, particularly for precise instance-level identification or fine-grained spatial reasoning [8, 35, 42]. These challenges highlight a fundamental gap between high-dimensional sensory observations and sparse, low-dimensional action outputs.

**Reasoning-Decomposed VLAs with Visual Overlays.** Recent works have explored using intermediate visual representations to guide robotic manipulation. One line of approaches combines GPT-like reasoning with traditional grasp or control modules in a training-free manner [1, 34], relying on the vision-language model to output precise grounding boxes. Another line trains VLAs to

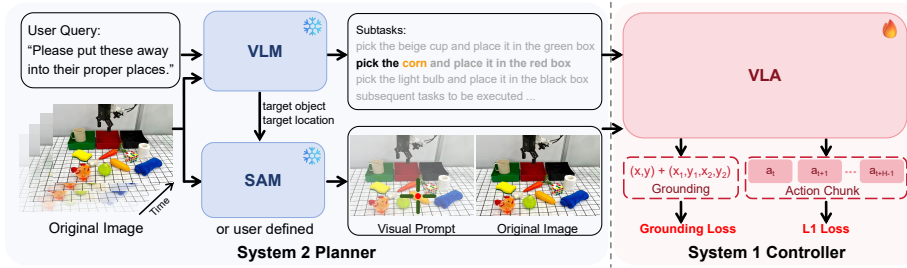


**Fig. 3:** Overall pipeline. VP-VLA leverages a dual-system architecture to bridge high-level reasoning and low-level control. The System 2 planner first decomposes a language instruction into subtasks and generates visual prompts as interaction anchors and spatial constraints. The System 1 controller then utilizes these grounded visual cues to generate precise sensorimotor trajectories for complex, multi-stage manipulation tasks, while a grounding loss aligns the policy with the highlighted regions during training.

predict intermediate affordances [20, 23], such as bounding boxes or trajectories, to inform downstream action policies. While effective in certain scenarios, these methods are limited: training-free pipelines suffer from low precision due to imperfect grounding, and end-to-end affordance prediction is difficult to train and may compromise reasoning capabilities, with no guarantee that predicted affordances translate to executable actions. In contrast, our framework separates subtask reasoning from low-level action execution by leveraging a pretrained VLM [37] for instruction decomposition and SAM3 [7] generated visual overlays as intermediate observations. This approach preserves the VLA’s native visual understanding and provides precise spatial guidance.

### 3 Method

We present **VP-VLA**, a decoupled dual-system framework for robotic manipulation. Following the problem formulation (Sec. 3.1), we propose two core components: (i) the System 2 planner  $P_{S2}$  (Sec. 3.2), an event-driven reasoning module that decomposes tasks into sub tasks and generates visual interface images; and (ii) the System 1 controller  $\pi_\theta$  (Sec. 3.3), a high-frequency controller that performs visuomotor tracking conditioned on these visual prompts.

#### 3.1 Preliminary

A standard VLA policy  $\pi_\theta$  typically maps a language instruction  $l$  and a sequence of visual observations  $o_t$  to a sequence of action  $a_t$  at each time step  $t$ . The number of visual observation,  $o_t = \{o_t^1, o_t^2, \dots, o_t^m\}$ , which came from a series of overhead or wrist-mounted camera, may vary depending on the embodiment. The sequence of action  $a_t = \{a_t^1, a_t^2, \dots, a_t^n\}$ , called action chunk, will be executed in sequence to compensate the inference delay and keep the execution smooth.  $a_t$

will be predicted as follows:

$$a_t = \pi_\theta(l, o_t), \quad (1)$$

where  $\pi_\theta$  is comprised of a pretrained VLM and an action decoder typically implemented as an MLP or a diffusion model.

Existing VLA models often suffer from a monolithic bottleneck, where a single network must concurrently manage instruction parsing, spatial reasoning, and motor execution. To address this, we propose VP-VLA, a decoupled dual-system architecture that bridges high-level reasoning and low-level control through an explicit visual interface.

### 3.2 System 2 Planner

The high-level System 2 planner,  $P_{S2}$ , performs deliberative reasoning to obtain the visual interface  $I_{vp}^t$ . This module operates through two interconnected stages: (i) Event-Driven Task Decomposition, and (ii) Visual Prompt Generation.

**Event-Driven Task Decomposition.** Instead of performing computationally expensive high-level reasoning regardless of current progression of tasks [46],  $P_{S2}$  utilizes an event-driven execution loop. We hypothesize that manipulation tasks are composed of discrete semantic phases (e.g., grasp, putting down), and the transitions between these phases are marked by transition events. We define the transition event  $E$  as a change in the robot’s physical interaction state  $S_t$ . Formally, the high-level planner is invoked only when:

$$E_t = \mathbb{1}(|\phi(S_t) - \phi(S_{t-1})| > \epsilon), \quad (2)$$

where  $\phi$  is a state-mapping function. In our tabletop manipulation setting, we instantiate  $\phi$  as the gripper status. A change in the gripper state (open to closed or vice-versa) serves as a physical proxy for a semantic phase shift, triggering a re-evaluation of the visual prompt to reflect the next sub-goal (e.g., shifting from the target object to the placement destination).

**Visual Prompt Generation.** Once an event is triggered, a pretrained VLM planner processes the language instruction  $l$  and observation  $o_t$ , then reason about the subtask that needs to further operate, together with the corresponding target object and target location names from the scene. These names are then passed into a pretrained segmentation model to generate a visual interface image  $I_{vp}^t$ . This image serves as a spatial bridge, translating abstract language instructions into action affordances. The whole process can be decomposed into semantic reasoning and spatial grounding: In semantic reasoning stage, the planner identifies the current subtask  $s_k$  and the associated entities  $e \in \{e_{obj}, e_{loc}\}$ :

$$s_k, e_{obj}, e_{loc} = \text{VLMplanner}(l, o_t, S_t). \quad (3)$$

In spatial grounding stage, a segmentation model  $\mathcal{G}$  maps these entities to visual prompts  $\psi_t$ :

$$\psi_t = \mathcal{G}(o_t, e_{obj}, e_{loc}), \quad (4)$$

where  $\psi_t$  consists of an interaction anchor  $C \in \mathbb{R}^2$  denoted as a crosshair and a spatial constraint  $B \in \mathbb{R}^4$  represented as a bounding box. These visual prompts are then overlaid on the overhead camera observation to obtain  $I_{vp}^t$ . Unlike raw images,  $I_{vp}^t$  provides explicit geometric priors: For manipulation primitives (e.g., “pick”), the system generates a crosshair  $C$  at the object’s centroid as an anchor for interaction. This reduces the policy’s search space from the entire image to a localized region of interaction. For placement primitives, a bounding box  $B$  defines the spatial constraint for target placement. By representing these as explicit visual overlays, we transform the VLA’s task from “interpreting intent” to “visuomotor tracking” of the provided prompts. After obtaining the visual interface image  $I_{vp}^t$ , We feed it together with the original observation  $o_t$  into the System 1 controller  $\pi_\theta$ .

### 3.3 System 1 Controller

We extend the standard VLA formulation by introducing the visual prompt image  $I_{vp}^t$  at each step, serves as a spatial bridge between the high-level reasoning and grounding and the low-level robot’s execution. Our policy is defined as:

$$a_t = \pi_\theta(l, o_t, I_{vp}^t). \quad (5)$$

The VLA policy  $\pi_\theta$  consists of a VLM backbone  $f_\omega$ , which processes multimodal inputs into high-level embeddings, and an action decoder  $h_\psi$ , which maps these embeddings to continuous control signals. The policy is thus defined as:

$$a_t = \pi_\theta(l, o_t, I_{vp}^t) = h_\psi(f_\omega(l, o_t, I_{vp}^t)), \quad (6)$$

where  $\omega$  and  $\psi$  are the parameters of the VLM and the action decoder, respectively, and  $\theta = \{\omega, \psi\}$ .

**Training Objective.** A key challenge in visual prompting is ensuring the model treats the overlays as semantic anchors rather than extraneous image noise. To address this, we introduce a visual grounding objective that forces the model to internalize the spatial coordinates of the prompts. Our framework can be naturally extended with the auxiliary grounding task. During training, we add an auxiliary grounding task on only key frames (first frame and the frame where  $E_t = \mathbf{1}$ ). We formulate grounding as a classification task over discretized spatial bins. Following the design of Qwen-3-VL, we divide the image dimensions into  $N$  uniform bins, where  $N = 1000$ . For target object crosshair with its center located at  $(x, y)$ , we query the VLM inside the VLA  $\pi_\theta$  to predict the 2D location. For target location bounding box, we query the VLM to predict the location  $[x_1, y_1, x_2, y_2]$ . During training, the VLM  $f_\omega$  is queried to predict these discretized locations in a structured JSON format. We optimize this using a Cross-Entropy (CE) loss for grounding, which provides a sharper and more structured training signal than traditional MSE. We use L1 loss for action prediction. Critically, the grounding loss is backpropagated only through the VLM parameters  $\omega$ :

$$\mathcal{L}_{\text{total}} = \mathcal{L}_{\text{action}}(\theta) + \lambda \mathbf{1}_{\text{event}} \mathcal{L}_{\text{grounding}}(\omega), \quad (7)$$

where  $\lambda$  is the coefficient to balance VLA action prediction and visual prompt grounding. This auxiliary grounding loss ensures that the policy’s internal representations are explicitly aligned with the visual prompts rather than treating it as external noise, leading to more precise and robust manipulation.

**Data Preparation.** For better consistency and efficiency, we use rule-based approach to first decompose the original task into a subtask list. At key frames, a VLM predicts the current subtask from the list, along with the target object and (if applicable) target location. Using the predicted object and location names, we perform text-conditioned segmentation on all frames to obtain masks and bounding boxes before the next key frame. These annotations are then converted into visual prompts  $\psi$ : a crosshair placed at the centroid of the target object mask and a bounding box over the target placement region. Each processed episode is stored with per-frame masks, boxes, and VLM subtask records. Episodes with any failures are discarded to avoid introducing noisy supervision.

## 4 Experiment

We conduct extensive experiments to validate our method, both in simulation and real-world settings. First, we elaborate the implementation details (Section 4.1). We then assess the performance on simulation benchmark (Section 4.2, 4.3). Next, we examine real-robot performance on cluttered and under-specified manipulation tasks to study instruction-following and OOD generalization in real-world deployment (Section 4.4).

### 4.1 Implementation Details

We use Qwen3-VL-4B-Instruct [37] as the high-level planner and SAM3 [7] to obtain the visual prompt. We use the default segmentation threshold where detection threshold and mask threshold to be 0.5. We only keep the visual prompt with highest score for target object and target location respectively.

Our codebase is based on starVLA [9] framework, trained on 8 GPUs, and strictly follows the training and evaluation procedure to ensure reproducibility. We adopt QwenOFT architecture, which replace the Prismatic VLM [15] in OpenVLA-OFT [17] with Qwen3-VL-4B-Instruct. We use Qwen3-VL-4B-Instruct for System 2 Planner as well. We employ the AdamW optimizer with learning rate as  $1e-5$  for VLM and  $1e-4$  for the action model. We set the  $\lambda$  to be 0.1 when calculating loss.

### 4.2 Experiment on Robocasa Benchmark

we applied our pipeline to the Robocasa-GR1-Tabletop benchmark [28], a simulation framework with tabletop kitchen environment, consisting of 24 diverse tasks and in total 24,000 videos. These tasks involves multi-step complex pick and place interactions with varied attributes and geometries. We utilize the

Humanoid Robot Tabletop Manipulation subset from the PhysicalAI Robotics-GR00T-X-Embodiment-Sim [2] dataset, following [9, 24]. To guarantee reproducibility and statistical significance, we evaluate each task using 50 independent trials and report the average success rate.

The quantitative results on the RoboCasa Tabletop simulation benchmark are summarized in Table 1. Taking QwenOFT as the primary baseline, our method achieves a new state-of-the-art average success rate of 53.8%, outperforming QwenOFT (48.8%) by a clear margin of +5.0%. Our approach also surpasses other strong baselines, including Isaac-GR00T N1.5 (48.2%), Isaac-GR00T N1.6 (47.6%), QwenGR00T (47.8%), and QwenPI (43.9%). Notably, the improvement is particularly evident in the “PnP \* to \* Close” setting, where our method reaches 54.3%, significantly exceeding QwenOFT (43.7%) and all other competitors. We observed that for long complex instructions involving multiple steps and nonprehensile grasping, such as “pick up the wine, place it into the cabinet and close the cabinet”, the VLM reasoner successfully decompose the task into subtask list [*“pick up the wine”, “place the wine into the cabinet”, “close the cabinet”*]. In addition, it identifies the target object and the specific affordance required for the final action (the cabinet door). Furthermore, the reasoner accurately detects subtask transitions, ensuring the target object shifts from the “wine” to the “door” only after the wine has been successfully placed. We also observe consistent gains in several challenging novel generalization splits, such as “PnP Novel From Placemat To Plate” (70.0% vs. 52.0% for QwenOFT) and “PnP Novel From Tray To Plate” (66.0% vs. 56.0%), where the evaluation includes random initialized position, novel appearance, and distracting object and container. Our method not only improves overall task success rate but also enhances generalization for varying background, object attribute and position.

### 4.3 Experiment on SimplerEnv Benchmark

We utilize two large-scale subsets from the Open X-Embodiment (OXE) dataset: BridgeDataV2 [39] and Fractal [6]. The model is fine-tuned for 70k steps on 8 GPUs (batch size 32 per device). This benchmark includes four manipulation tasks: “Put spoon on towel”, “Put carrot on plate”, “Stack green cube on yellow cube”, and “Put eggplant in yellow basket”. We evaluate the policies using the official evaluation scripts provided by the SimplerEnv repository [22].

The quantitative results on the SimplerEnv simulation benchmark are summarized in Table 2. Using QwenOFT as the primary baseline (50.0% average), our method achieves a new state-of-the-art performance of 58.3%, yielding a substantial improvement of +8.3%. Compared with other strong competitors, our approach also surpasses  $\pi_{0.5}$  (57.1%) and Isaac-GR00T-N1.6-Bridge (57.1%), and outperforms prior VLA systems such as CogACT (51.3%) and VideoVLA (53.1%). At the task level, we observe notable improvements over QwenOFT in tasks requiring precise object identification, manipulation and target location grounding, including “Put Spoon on Towel” (66.7% vs. 58.3%) and a substantial gain in “Put Eggplant in Yellow Basket” (95.8% vs. 70.8%). These findings suggest that our approach more effectively leverages language-conditioned signals to

**Table 1:** Results of evaluating the VLA models with the GR1 robot in the RoboCasa Tabletop simulation environment. The results are sourced from the official IsaacGR00T github repository [2] and starVLA community [9]. We highlight the best result in **bold** and the second-best results with underline.

Task	Isaac-GR00T N1.5	Isaac-GR00T N1.6	QwenGR00T +Qwen3VL	QwenPI +Qwen3VL	QwenOFT +Qwen3VL	QwenFAST +Qwen3VL	Ours +Qwen3VL
PnP Bottle To Cabinet Close	54.0	51.5	46.0	26.0	30.0	38.0	54.0
PnP Can To Drawer Close	50.0	13.0	80.0	62.0	76.0	44.0	72.0
PnP Cup To Drawer Close	38.0	8.5	54.0	42.0	44.0	56.0	44.0
PnP Milk To Microwave Close	60.0	14.0	48.0	50.0	44.0	44.0	74.0
PnP Potato To Microwave Close	32.0	41.5	28.0	42.0	32.0	14.0	34.0
PnP Wine To Cabinet Close	38.0	16.5	46.0	32.0	36.0	14.0	48.0
<b>PnP * to * Close (Avg)</b>	45.3	24.2	50.3	42.3	43.7	35.0	54.3
PnP Novel From Cuttingboard To Basket	38.0	58.0	48.0	40.0	50.0	54.0	66.0
PnP Novel From Cuttingboard To Cardboardbox	46.0	46.5	40.0	46.0	40.0	42.0	54.0
PnP Novel From Cuttingboard To Pan	58.0	68.5	68.0	60.0	70.0	58.0	74.0
PnP Novel From Cuttingboard To Pot	62.0	65.0	52.0	40.0	54.0	58.0	54.0
PnP Novel From Cuttingboard To Tieredbasket	28.0	46.5	56.0	44.0	38.0	40.0	56.0
<b>PnP Novel From Cuttingboard To * (Avg)</b>	46.4	56.9	52.8	46.0	50.4	50.4	60.8
PnP Novel From Placemat To Basket	30.0	58.5	42.0	44.0	32.0	36.0	48.0
PnP Novel From Placemat To Bowl	60.0	57.5	44.0	52.0	58.0	38.0	74.0
PnP Novel From Placemat To Plate	56.0	63.0	48.0	50.0	52.0	42.0	70.0
PnP Novel From Placemat To Tieredshelf	36.0	28.5	18.0	28.0	24.0	18.0	26.0
<b>PnP Novel From Placemat To * (Avg)</b>	45.5	51.9	38.0	43.5	41.5	33.5	54.5
PnP Novel From Tray To Cardboardbox	52.0	51.5	38.0	34.0	44.0	28.0	44.0
PnP Novel From Tray To Plate	48.0	71.0	56.0	64.0	56.0	34.0	66.0
PnP Novel From Tray To Pot	60.0	64.5	50.0	44.0	62.0	46.0	38.0
PnP Novel From Tray To Tieredbasket	52.0	57.0	36.0	50.0	54.0	36.0	58.0
PnP Novel From Tray To Tieredshelf	32.0	31.5	16.0	28.0	30.0	16.0	24.0
<b>PnP Novel From Tray To * (Avg)</b>	48.8	55.1	39.2	44.0	49.2	32.0	46.0
PnP Novel From Plate To Bowl	58.0	57.0	60.0	52.0	60.0	52.0	52.0
PnP Novel From Plate To Cardboardbox	44.0	43.5	50.0	40.0	50.0	30.0	44.0
PnP Novel From Plate To Pan	60.0	51.0	54.0	36.0	66.0	48.0	56.0
PnP Novel From Plate To Plate	64.0	78.7	70.0	48.0	68.0	50.0	62.0
<b>PnP Novel From Plate To * (Avg)</b>	56.5	57.6	58.5	44.0	61.0	45.0	53.5
<b>Average</b>	48.2	47.6	47.8	43.9	<u>48.8</u>	39.0	<b>53.8</b>

guide action selection, leading to consistent improvements over QwenOFT and establishing a new performance ceiling on this benchmark.

#### 4.4 Experiment on Real-world Scenario

We comprehensively evaluate VP-VLA across multiple real-world manipulation tasks to validate its core capabilities in several dimensions. Specifically, we focus on: (i) the reasoning and grounding ability within cluttered scenes reflected on overall success rates; (ii) the robustness and generalization ability in out-of-distribution (OOD) settings; and (iii) the effectiveness of visual prompting against textual prompting in scenarios requiring complex spatial reasoning.

**Table 2:** Results of evaluating the VLA models with the WidowX robot in the SimpleEnv simulation environment. We highlight the best results in **bold** and the second-best results with underline.

Method	Put Spoon on Towel	Put Carrot on Plate	Stack Green Block on Yellow Block	Put Eggplant in Yellow Basket	Average
RT-1-X [30]	0.0	4.2	0.0	0.0	1.1
Octo-Base [36]	15.8	12.5	0.0	41.7	17.5
Octo-Small [36]	41.7	8.2	0.0	56.7	26.7
OpenVLA-OFT [17]	34.2	30.0	30.0	72.5	41.8
RoboVLM [26]	50.0	37.5	0.0	83.3	42.7
Magma [41]	37.5	29.2	20.8	91.7	44.8
CogACT [21]	71.7	50.8	15.0	67.5	51.3
SpatialVLA [31]	20.8	20.8	25.0	70.8	34.4
TraceVLA [45]	12.5	16.6	16.6	65.0	27.7
VideoVLA [32]	75.0	20.8	45.8	70.8	53.1
$\pi_0$ [3]	29.2	62.5	29.2	91.6	53.1
$\pi_{0.5}$ [12]	49.3	64.7	44.7	69.7	<u>57.1</u>
Isaac-GR00T-N1.6-Bridge [2]	64.5	65.5	5.5	93.0	<u>57.1</u>
QwenOFT + Qwen3VL	58.3	50.0	20.8	70.8	50.0
Ours + Qwen3VL	66.7	50.0	20.8	95.8	<b>58.3</b>

For each of the following section, we introduce our experimental setup and evaluation results. We use a stationary, table-mounted Franka Research 3 7-DoF robot arm. Environment observation includes two RGB images: one from a fixed third-person perspective and the other from a first-person camera mounted on the end-effector. The setup is shown in 4. Both images are resized to  $224 \times 224$  before feeding into the model. We fine-tune both the baseline model and our method using 8 GPUs, with total batch size of 256 and action chunk size of 16.

**Robotic Waste-Sorting Categorization.** To evaluate visual grounding and generalization in cluttered environments, we design a robotic pick-and-place task inspired by daily waste-sorting scenarios. Models must follow instructions to categorize randomly posed objects into specific containers, which requires both visual grounding ability and precise action prediction. We collect 50 trajectories per training object and evaluate both our method and the QwenOFT baseline at 10K training steps. We evaluate performance across In-Domain (ID) setting and out-of-distribution setting (OOD) with novel object.

As shown in Table 3, our method achieves an 87.5% ID success rate and 85% OOD success rate, significantly outperforming QwenOFT (80% ID, 63.3% OOD). Notably, our method exhibits a minimal generalization gap (2.5%), whereas QwenOFT suffers a 16.7% performance drop. This suggests that while the baseline overfits to the training distribution, our approach maintains robust object-level grounding across categories in cluttered scenes.

We further analyze the performance for each boxes: (i) In the Green Box (Recyclable), QwenOFT struggled with a red shoe (7/10), suggesting a reliance on color heuristics. Our model remained robust (9/10), demonstrating category grounding independent of surface appearance. (ii) For the Red Box (Kitchen Waste), our model maintained 85% accuracy on novel OOD objects (pear, carrot)

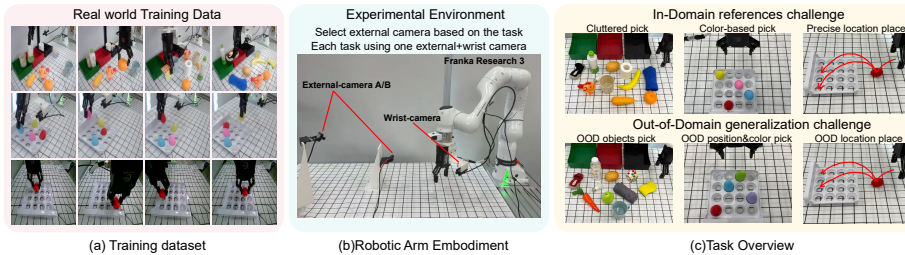


**Fig. 4:** Overviews of our real-world task and robot setting. (a) We collect real-world robot demonstration for three task suites. (b) Robot setting for the experiments. We use external camera A for categorization task and pick colored egg task, while using external camera B for egg carton placement task. (c) We present examples of each task with the OOD setting illustration.

**Table 3:** Categorization results (10k steps). Successes out of 10 trials. Bold indicates best performance.

Object	Ours	QwenOFT	Object	Ours	QwenOFT
<i>Green Box</i>			<i>Red Box</i>		
Bottle (ID)	7	7	Banana (ID)	8	6
Beige cup (ID)	9	8	Orange (ID)	9	9
Black shoe (ID)	10	9	Corn (ID)	10	9
Toy chicken (ID)	8	7	Potato (ID)	10	10
Blue cup (OOD)	8	8	Pear (OOD)	9	8
Red shoe (OOD)	9	7	Carrot (OOD)	8	7
<i>Black Box</i>			<b>Summary Statistics</b>		
Towel (ID)	10	10	<b>Summary</b>	<b>ID/OOD</b>	<b>ID/OOD</b>
Light bulb (ID)	6	4	<b>Green Avg</b>	34/17	31/15
Rubik’s cube (ID)	10	9	<b>Red Avg</b>	37/17	34/15
Toilet paper (ID)	8	8	<b>Black Avg</b>	34/17	31/8
Scrambled cube (OOD)	9	3	<b>Total ID</b>	<b>87.5%</b>	80.0%
Sponge (OOD)	8	5	<b>Total OOD</b>	<b>85.0%</b>	63.3%

compared to 75% for the baseline, reflecting superior semantic abstraction. (iii) The Black Box (Other Waste) highlighted the largest gap. On scrambled Rubik’s cubes, which share semantic identity with the training set but differ visually, QwenOFT’s performance collapsed (3/10) due to imprecise grasping and pattern overfitting. Our method achieved 9/10 by strictly following visual prompts and grounding the object to the correct placement location, even for challenging OOD items like sponge (8/10 vs. 5/10), where the baseline appears not knowing which box to place the object.

**Object Reference by Attribute.** To evaluate fine-grained attribute grounding, we design a color-based reference task: “pick up the  $\langle color \rangle$  egg.” Unlike category-level reasoning in the previous experiment, this task focuses on attribute-level grounding, requiring the model to bind specific linguistic color tokens to visual instances under spatial variation. Using a  $4 \times 4$  grid, we collect

**Table 4:** Pick colored egg results. Performance (raw score/12) of our method vs. QwenOFT. We evaluate across In-Domain (ID) and two OOD scenarios (Color and Position change).

Color	In-Domain		OOD (Color)		OOD (Pos.)			
	Ours	QwenOFT	Ours	QwenOFT	Ours	QwenOFT		
Blue	10	7						
Pink	8	6	Purple	9	4	Blue	9	6
Red	10	8	Green	9	3	Red	9	7
Yellow	9	7						
<b>Avg (%)</b>	<b>77.1</b>	58.3		<b>75.0</b>	29.2		<b>75.0</b>	54.2

200 demonstrations (50 per color for blue, pink, red, and yellow). We evaluate performance across three settings: In-Domain (ID), OOD Color (novel purple and green eggs), and OOD Position (eggs placed in 12 unseen grid locations).

Table 4 summarizes the performance across all settings. Our method significantly outperforms the baseline, particularly under distribution shifts. For in-domain scenario, our model achieves 77.1% accuracy, outperforming the baseline by a large margin of 18.8%. For OOD Color scenario, our method maintains 75.0% success on novel colors, while the baseline drops to 29.2%. The minimal gap between our ID and OOD color performance (2.1%) suggests the learned representation captures attribute semantics rather than memorizing instances. In contrast, the baseline exhibits severe overfitting to seen color distributions. Finally, for OOD position with unseen grid locations, our model reaches 75.0% compared to 54.2% for the baseline, demonstrating spatial generalization beyond training data, while the baseline shows weaker position invariance.

We further analyze the performance for each configuration: (i) ID Colors: our method consistently surpasses baseline across all training colors. Failures in baseline often involve imprecise grasp positioning or failing to move above the target-colored egg, indicating weaker visuomotor alignment for attribute-conditioned manipulations. (ii) OOD Color: The baseline frequently confuses novel colors with visually similar training colors or defaults to the egg closest to the gripper while ignoring the color condition. In contrast, our model consistently moves accurately to the target, achieving 9/12 for both colors. This suggests better disentanglement between linguistic attributes and spatial proximity bias. (iii) OOD Position: For eggs placed at unseen positions, the baseline shows a bias toward previously demonstrated columns, indicating spatial memorization. Our model achieves 9/12 for both colored eggs, demonstrating spatial generalization and more stable grasping under positional shift.

**Location reference with spatial grounding.** To evaluate precise spatial reasoning, we design an egg carton placement task. The robot must pick up an egg and place it at a language-specified coordinate (e.g., “line 2, column 4”) on a 4×4 grid. We manually drawn target location visual prompt (bounding box) at the target location for our method to resolve potential linguistic ambiguity, whereas the baseline must ground the instruction purely from text. We evaluate

**Table 5:** Egg carton placement results. Successes are reported out of 5 trials.  $LX$   $CY$  denotes the position at Line  $X$ , Column  $Y$ . We report both In-Domain (ID) and Out-of-Distribution (OOD) performance.

In-Domain (ID)			Out-of-Distribution (OOD)		
Pos.	Ours	QwenOFT	Pos.	Ours	QwenOFT
L1 C2	5.00	4.25	L1 C3	2.50	1.75
L1 C4	5.00	4.50	L2 C1	2.25	2.50
L2 C4	5.00	2.25	L3 C2	5.00	3.25
L2 C2	4.00	4.25	L4 C3	4.00	3.50
L3 C1	4.50	4.50	<b>Summary Statistics</b>		
L3 C3	4.50	1.00	<b>Group</b>	<b>Ours</b>	<b>QwenOFT</b>
L4 C2	4.50	3.00	ID Avg.	<b>91.3%</b>	70.6%
L4 C4	4.00	4.50	OOD Avg.	<b>68.8%</b>	55.0%

on In-Domain (ID) and Out-of-Distribution (OOD) coordinates using a partial credit system: 1.0 for the target cell, 0.5 for adjacent, and 0.25 for diagonal cells.

As shown in Table 5, our method consistently outperforms QwenOFT across all settings: For In-Domain setting, our model achieves 91.25% accuracy (36.5/40), a more than 20% improvement over QwenOFT (70.63%). This reflects stable spatial grounding when coordinates are seen during training. For out-of-distribution scenario with novel row-column combinations, our method reaches 68.75%, compared to 55% for the baseline. While OOD compositional generalization is challenging for both, our model maintains a significant performance lead, suggesting superior geometric grounding over memorization of frequently seen coordinates.

We further analyze the performance for each configuration: (i) In-Domain Positions: Our model achieves near-perfect scores on most ID coordinates, indicating accurate row-column parsing. Conversely, QwenOFT shows high variance; for instance, it drops to 1/5 at L3C3 (vs. our 4.5/5), struggling to resolve spatial references when vertical and horizontal axes must be composed jointly. (ii) Out-of-Distribution Positions: OOD tasks require the model to follow target masks at coordinates never jointly observed during training. Our method maintains strong performance at L3C2 (5/5) and L4C3 (4/5), successfully extending the visual-prompt-following mechanism to new locations. QwenOFT remains inconsistent (1.75/5 to 3.5/5), often failing to generalize the underlying grid geometry to novel index combinations.

#### 4.5 Ablation Study

We conduct ablation experiments on the RoboCasa Tabletop simulation to analyze the contribution of each design component. Table 1 reports the results.

**Effect of the Grounding Objective.** Removing the grounding loss (“w/o grounding”) reduces the overall success rate from 53.8% to 49.4%, demonstrating that explicitly aligning policy representations with the prompted regions is crucial. Without this constraint, the model may perceive the visual prompts

**Table 6:** Ablation results of evaluating the VLA models with the GR1 robot in the RoboCasa Tabletop simulation environment

Task	w/o grounding	w/ all frame grounding	w/ point	w/ direct overlay	Ours (Full)
PnP * to * Close (Avg)	49.7	46.3	38.7	47.7	54.3
PnP Novel From Cuttingboard To * (Avg)	54.4	53.6	48.8	54.0	60.8
PnP Novel From Placemat To * (Avg)	46.0	45.0	46.0	46.5	54.5
PnP Novel From Tray To * (Avg)	43.2	46.0	49.6	50.0	46.0
PnP Novel From Plate To * (Avg)	54.0	58.0	56.5	56.5	53.5
<b>Average</b>	49.4	49.5	47.3	50.8	53.8

but fail to consistently associate them with action generation. We further evaluate grounding applied to every frame (“w/ all frame grounding”). This variant achieves 49.5%, which is lower than our key-frame grounding strategy. Applying grounding supervision densely across all frames may introduce redundant or noisy constraints, leading to unstable training and suboptimal optimization. This result suggests that selective grounding at key decision frames provides a better balance between supervision strength and training stability.

**Effect of Visual Prompt Design.** Changing the target object prompt from a crosshair to a point (“w/ point”) degrades performance to 47.3% on average. A single point provides weaker spatial extent information compared to a structured crosshair, making it harder for the policy to infer object location but rather treating it as visual perturbation. This indicates that prompt geometry influences how effectively spatial cues are interpreted. We also test directly overlaying prompts on the primary RGB image (“w/ direct overlay”), which yields 50.8%. Separating the visual prompt avoids excessive interference with raw visual features and prevent overlapping.

**Overall Discussion.** Across all variants, our full method consistently achieves the best across all tasks. The results demonstrate that (i) grounding supervision is necessary for reliable prompt utilization, (ii) supervision should be applied selectively rather than densely, and (iii) prompt representation design significantly affects perception. Together, these findings validate the current design.

## 5 Conclusion

This paper presents VP-VLA, a novel dual-system vision-language-action framework. By decoupling high-level reasoning from low-level execution, our approach leverages a “System 2 Planner” to translate complex linguistic instructions into explicit, structured visual prompts, including cross-hairs and bounding boxes. These spatial anchors, combined with an auxiliary visual grounding objective during training, effectively guide the “System 1 Controller” to perform precise

manipulation tasks. Extensive evaluations across simulated benchmarks, including Robocasa-GR1-Tabletop and SimplerEnv, as well as real-world cluttered scenarios, demonstrate the superior performance of VP-VLA.

## References

1. Ahn, M., Brohan, A., Brown, N., Chebotar, Y., Cortes, O., David, B., Finn, C., Fu, C., Gopalakrishnan, K., Hausman, K., Herzog, A., Ho, D., Hsu, J., Ibarz, J., Ichter, B., Irpan, A., Jang, E., Ruano, R.J., Jeffrey, K., Jesmonth, S., Joshi, N.J., Julian, R., Kalashnikov, D., Kuang, Y., Lee, K.H., Levine, S., Lu, Y., Luu, L., Parada, C., Pastor, P., Quiambao, J., Rao, K., Rettinghouse, J., Reyes, D., Sermanet, P., Sievers, N., Tan, C., Toshev, A., Vanhoucke, V., Xia, F., Xiao, T., Xu, P., Xu, S., Yan, M., Zeng, A.: Do as i can, not as i say: Grounding language in robotic affordances (2022), <https://arxiv.org/abs/2204.01691>
2. Bjorck, J., Castañeda, F., Cherniadev, N., Da, X., Ding, R., Fan, L., Fang, Y., Fox, D., Hu, F., Huang, S., et al.: Gr00t n1: An open foundation model for generalist humanoid robots. arXiv preprint arXiv:2503.14734 (2025)
3. Black, K., Brown, N., Driess, D., Esmail, A., Equi, M., Finn, C., Fusai, N., Groom, L., Hausman, K., Ichter, B., et al.:  $\pi_0$ : A vision-language-action flow model for general robot control. arXiv preprint arXiv:2410.24164 (2024)
4. Brohan, A., Brown, N., Carbajal, J., Chebotar, Y., Chen, X., Choromanski, K., Ding, T., Driess, D., Dubey, A., Finn, C., Florence, P., Fu, C., Arenas, M.G., Gopalakrishnan, K., Han, K., Hausman, K., Herzog, A., Hsu, J., Ichter, B., Irpan, A., Joshi, N., Julian, R., Kalashnikov, D., Kuang, Y., Leal, I., Lee, L., Lee, T.W.E., Levine, S., Lu, Y., Michalewski, H., Mordatch, I., Pertsch, K., Rao, K., Reymann, K., Ryoo, M., Salazar, G., Sanketi, P., Sermanet, P., Singh, J., Singh, A., Soricut, R., Tran, H., Vanhoucke, V., Vuong, Q., Wahid, A., Welker, S., Wohlhart, P., Wu, J., Xia, F., Xiao, T., Xu, P., Xu, S., Yu, T., Zitkovich, B.: Rt-2: Vision-language-action models transfer web knowledge to robotic control (2023), <https://arxiv.org/abs/2307.15818>
5. Brohan, A., Brown, N., Carbajal, J., Chebotar, Y., Dabis, J., Finn, C., Gopalakrishnan, K., Hausman, K., Herzog, A., Hsu, J., Ibarz, J., Ichter, B., Irpan, A., Jackson, T., Jesmonth, S., Joshi, N.J., Julian, R., Kalashnikov, D., Kuang, Y., Leal, I., Lee, K.H., Levine, S., Lu, Y., Malla, U., Manjunath, D., Mordatch, I., Nachum, O., Parada, C., Peralta, J., Perez, E., Pertsch, K., Quiambao, J., Rao, K., Ryoo, M., Salazar, G., Sanketi, P., Sayed, K., Singh, J., Sontakke, S., Stone, A., Tan, C., Tran, H., Vanhoucke, V., Vega, S., Vuong, Q., Xia, F., Xiao, T., Xu, P., Xu, S., Yu, T., Zitkovich, B.: Rt-1: Robotics transformer for real-world control at scale (2023), <https://arxiv.org/abs/2212.06817>
6. Brohan, A., Brown, N., Carbajal, J., Chebotar, Y., Dabis, J., Finn, C., Gopalakrishnan, K., Hausman, K., Herzog, A., Hsu, J., et al.: Rt-1: Robotics transformer for real-world control at scale. arXiv preprint arXiv:2212.06817 (2022)
7. Carion, N., Gustafson, L., Hu, Y.T., Debnath, S., Hu, R., Suris, D., Ryali, C., Alwala, K.V., Khedr, H., Huang, A., Lei, J., Ma, T., Guo, B., Kalla, A., Marks, M., Greer, J., Wang, M., Sun, P., Rädle, R., Afouras, T., Mavroudi, E., Xu, K., Wu, T.H., Zhou, Y., Momeni, L., Hazra, R., Ding, S., Vaze, S., Porcher, F., Li, F., Li, S., Kamath, A., Cheng, H.K., Dollár, P., Ravi, N., Saenko, K., Zhang, P., Feichtenhofer, C.: Sam 3: Segment anything with concepts (2025), <https://arxiv.org/abs/2511.16719>

8. Chen, W., Belkhale, S., Mirchandani, S., Mees, O., Driess, D., Pertsch, K., Levine, S.: Training strategies for efficient embodied reasoning (2025), <https://arxiv.org/abs/2505.08243>
9. starVLA Contributors: Starvla: A lego-like codebase for vision-language-action model developing. GitHub repository (1 2025). <https://doi.org/10.5281/zenodo.18264214>, <https://github.com/starVLA/starVLA>
10. Fei, S., Wang, S., Shi, J., Dai, Z., Cai, J., Qian, P., Ji, L., He, X., Zhang, S., Fei, Z., et al.: Libero-plus: In-depth robustness analysis of vision-language-action models. arXiv preprint arXiv:2510.13626 (2025)
11. He, W., Dai, Y., Zheng, Y., Wu, Y., Cao, Z., Liu, D., Jiang, P., Yang, M., Huang, F., Si, L., Sun, J., Li, Y.: Galaxy: A generative pre-trained model for task-oriented dialog with semi-supervised learning and explicit policy injection (2022), <https://arxiv.org/abs/2111.14592>
12. Intelligence, P., Black, K., Brown, N., Darpinian, J., Dhabalia, K., Driess, D., Esmail, A., Equi, M., Finn, C., Fusai, N., et al.:  $\pi_{0.5}$ : a vision-language-action model with open-world generalization. arXiv preprint arXiv:2504.16054 (2025)
13. Jones, J., Mees, O., Sferrazza, C., Stachowicz, K., Abbeel, P., Levine, S.: Beyond sight: Finetuning generalist robot policies with heterogeneous sensors via language grounding (2025), <https://arxiv.org/abs/2501.04693>
14. Kahneman, D.: Thinking, fast and slow. macmillan (2011)
15. Karamcheti, S., Nair, S., Balakrishna, A., Liang, P., Kollar, T., Sadigh, D.: Prismatic vlms: Investigating the design space of visually-conditioned language models. In: Forty-first International Conference on Machine Learning (2024)
16. Khazatsky, A., Pertsch, K., Nair, S., Balakrishna, A., Dasari, S., Karamcheti, S., Nasiriany, S., Srirama, M.K., Chen, L.Y., Ellis, K., Fagan, P.D., Hejna, J., Itkina, M., Lepert, M., Ma, Y.J., Miller, P.T., Wu, J., Belkhale, S., Dass, S., Ha, H., Jain, A., Lee, A., Lee, Y., Memmel, M., Park, S., Radosavovic, I., Wang, K., Zhan, A., Black, K., Chi, C., Hatch, K.B., Lin, S., Lu, J., Mercat, J., Rehman, A., Sanketi, P.R., Sharma, A., Simpson, C., Vuong, Q., Walke, H.R., Wulfe, B., Xiao, T., Yang, J.H., Yavary, A., Zhao, T.Z., Agia, C., Baijal, R., Castro, M.G., Chen, D., Chen, Q., Chung, T., Drake, J., Foster, E.P., Gao, J., Guizilini, V., Herrera, D.A., Heo, M., Hsu, K., Hu, J., Irshad, M.Z., Jackson, D., Le, C., Li, Y., Lin, K., Lin, R., Ma, Z., Maddukuri, A., Mirchandani, S., Morton, D., Nguyen, T., O'Neill, A., Scalise, R., Seale, D., Son, V., Tian, S., Tran, E., Wang, A.E., Wu, Y., Xie, A., Yang, J., Yin, P., Zhang, Y., Bastani, O., Berseth, G., Bohg, J., Goldberg, K., Gupta, A., Gupta, A., Jayaraman, D., Lim, J.J., Malik, J., Martín-Martín, R., Ramamoorthy, S., Sadigh, D., Song, S., Wu, J., Yip, M.C., Zhu, Y., Kollar, T., Levine, S., Finn, C.: Droid: A large-scale in-the-wild robot manipulation dataset (2025), <https://arxiv.org/abs/2403.12945>
17. Kim, M.J., Finn, C., Liang, P.: Fine-tuning vision-language-action models: Optimizing speed and success. arXiv preprint arXiv:2502.19645 (2025)
18. Kim, M.J., Pertsch, K., Karamcheti, S., Xiao, T., Balakrishna, A., Nair, S., Rafailov, R., Foster, E., Lam, G., Sanketi, P., Vuong, Q., Kollar, T., Burchfiel, B., Tedrake, R., Sadigh, D., Levine, S., Liang, P., Finn, C.: Openvla: An open-source vision-language-action model (2024), <https://arxiv.org/abs/2406.09246>
19. Lee, S., Mo, S., Han, W.S.: Bring my cup! personalizing vision-language-action models with visual attentive prompting. arXiv preprint arXiv:2512.20014 (2025)
20. Li, J., Zhu, Y., Tang, Z., Wen, J., Zhu, M., Liu, X., Li, C., Cheng, R., Peng, Y., Peng, Y., et al.: Coa-vla: Improving vision-language-action models via visual-textual chain-of-affordance. arXiv preprint arXiv:2412.20451 (2024)

21. Li, Q., Liang, Y., Wang, Z., Luo, L., Chen, X., Liao, M., Wei, F., Deng, Y., Xu, S., Zhang, Y., et al.: Cogact: A foundational vision-language-action model for synergizing cognition and action in robotic manipulation. arXiv preprint arXiv:2411.19650 (2024)
22. Li, X., Hsu, K., Gu, J., Pertsch, K., Mees, O., Walke, H.R., Fu, C., Lunawat, I., Sieh, I., Kirmani, S., et al.: Evaluating real-world robot manipulation policies in simulation. arXiv preprint arXiv:2405.05941 (2024)
23. Li, Y., Deng, Y., Zhang, J., Jang, J., Memmel, M., Yu, R., Garrett, C.R., Ramos, F., Fox, D., Li, A., et al.: Hamster: Hierarchical action models for open-world robot manipulation. arXiv preprint arXiv:2502.05485 (2025)
24. Lian, S., Yu, B., Lin, X., Yang, L.T., Shen, Z., Wu, C., Miao, Y., Huang, C., Chen, K.: Bayesianvla: Bayesian decomposition of vision language action models via latent action queries. arXiv preprint arXiv:2601.15197 (2026)
25. Liu, B., Zhu, Y., Gao, C., Feng, Y., Liu, Q., Zhu, Y., Stone, P.: Libero: Benchmarking knowledge transfer for lifelong robot learning (2023), <https://arxiv.org/abs/2306.03310>
26. Liu, H., Li, X., Li, P., Liu, M., Wang, D., Liu, J., Kang, B., Ma, X., Kong, T., Zhang, H.: Towards generalist robot policies: What matters in building vision-language-action models (2025)
27. Liu, S., Wu, L., Li, B., Tan, H., Chen, H., Wang, Z., Xu, K., Su, H., Zhu, J.: Rdt-1b: a diffusion foundation model for bimanual manipulation. arXiv preprint arXiv:2410.07864 (2024)
28. Nasiriany, S., Maddukuri, A., Zhang, L., Parikh, A., Lo, A., Joshi, A., Mandlekar, A., Zhu, Y.: Robocasa: Large-scale simulation of everyday tasks for generalist robots. arXiv preprint arXiv:2406.02523 (2024)
29. OpenAI, Achiam, J., Adler, S., Agarwal, S., Ahmad, L., Akkaya, I., Aleman, F.L., Almeida, D., Altenschmidt, J., Altman, S., Anadkat, S., Avila, R., Babuschkin, I., Balaji, S., Balcom, V., Baltescu, P., Bao, H., Bavarian, M., Belgum, J., Bello, I., Berdine, J., Bernadett-Shapiro, G., Berner, C., Bogdonoff, L., Boiko, O., Boyd, M., Brakman, A.L., Brockman, G., Brooks, T., Brundage, M., Button, K., Cai, T., Campbell, R., Cann, A., Carey, B., Carlson, C., Carmichael, R., Chan, B., Chang, C., Chantzis, F., Chen, D., Chen, S., Chen, R., Chen, J., Chen, M., Chess, B., Cho, C., Chu, C., Chung, H.W., Cummings, D., Currier, J., Dai, Y., Decareaux, C., Degry, T., Deutsch, N., Deville, D., Dhar, A., Dohan, D., Dowling, S., Dunning, S., Ecoffet, A., Eleti, A., Eloundou, T., Farhi, D., Fedus, L., Felix, N., Fishman, S.P., Forte, J., Fulford, I., Gao, L., Georges, E., Gibson, C., Goel, V., Gogineni, T., Goh, G., Gontijo-Lopes, R., Gordon, J., Grafstein, M., Gray, S., Greene, R., Gross, J., Gu, S.S., Guo, Y., Hallacy, C., Han, J., Harris, J., He, Y., Heaton, M., Heidecke, J., Hesse, C., Hickey, A., Hickey, W., Hoeschele, P., Houghton, B., Hsu, K., Hu, S., Hu, X., Huizinga, J., Jain, S., Jain, S., Jang, J., Jiang, A., Jiang, R., Jin, H., Jin, D., Jomoto, S., Jonn, B., Jun, H., Kaftan, T., Łukasz Kaiser, Kamali, A., Kanitscheider, I., Keskar, N.S., Khan, T., Kilpatrick, L., Kim, J.W., Kim, C., Kim, Y., Kirchner, J.H., Kiros, J., Knight, M., Kokotajlo, D., Łukasz Kondraciuk, Kondrich, A., Konstantinidis, A., Kosic, K., Krueger, G., Kuo, V., Lampe, M., Lan, I., Lee, T., Leike, J., Leung, J., Levy, D., Li, C.M., Lim, R., Lin, M., Lin, S., Litwin, M., Lopez, T., Lowe, R., Lue, P., Makanju, A., Malfacini, K., Manning, S., Markov, T., Markovski, Y., Martin, B., Mayer, K., Mayne, A., McGrew, B., McKinney, S.M., McLeavey, C., McMillan, P., McNeil, J., Medina, D., Mehta, A., Menick, J., Metz, L., Mishchenko, A., Mishkin, P., Monaco, V., Morikawa, E., Mossing, D., Mu, T., Murati, M., Murk, O., Mély, D., Nair, A., Nakano, R., Nayak,

- R., Neelakantan, A., Ngo, R., Noh, H., Ouyang, L., O’Keefe, C., Pachocki, J., Paino, A., Palermo, J., Pantuliano, A., Parascandolo, G., Parish, J., Parparita, E., Passos, A., Pavlov, M., Peng, A., Perelman, A., de Avila Belbute Peres, F., Petrov, M., de Oliveira Pinto, H.P., Michael, Pokorny, Pokrass, M., Pong, V.H., Powell, T., Power, A., Power, B., Proehl, E., Puri, R., Radford, A., Rae, J., Ramesh, A., Raymond, C., Real, F., Rimbach, K., Ross, C., Rotsted, B., Roussez, H., Ryder, N., Saltarelli, M., Sanders, T., Santurkar, S., Sastry, G., Schmidt, H., Schnurr, D., Schulman, J., Selsam, D., Sheppard, K., Sherbakov, T., Shieh, J., Shoker, S., Shyam, P., Sidor, S., Sigler, E., Simens, M., Sitkin, J., Slama, K., Sohl, I., Sokolowsky, B., Song, Y., Staudacher, N., Such, F.P., Summers, N., Sutskever, I., Tang, J., Tezak, N., Thompson, M.B., Tillet, P., Tootoonchian, A., Tseng, E., Tuggle, P., Turley, N., Tworek, J., Uribe, J.F.C., Vallone, A., Vijayvergiya, A., Voss, C., Wainwright, C., Wang, J.J., Wang, A., Wang, B., Ward, J., Wei, J., Weinmann, C., Welihinda, A., Welinder, P., Weng, J., Weng, L., Wiethoff, M., Willner, D., Winter, C., Wolrich, S., Wong, H., Workman, L., Wu, S., Wu, J., Wu, M., Xiao, K., Xu, T., Yoo, S., Yu, K., Yuan, Q., Zaremba, W., Zellers, R., Zhang, C., Zhang, M., Zhao, S., Zheng, T., Zhuang, J., Zhuk, W., Zoph, B.: Gpt-4 technical report (2024), <https://arxiv.org/abs/2303.08774>
30. O’Neill, A., Rehman, A., Maddukuri, A., Gupta, A., Padalkar, A., Lee, A., Pooley, A., Gupta, A., Mandlekar, A., Jain, A., et al.: Open x-embodiment: Robotic learning datasets and rt-x models: Open x-embodiment collaboration 0. In: 2024 IEEE International Conference on Robotics and Automation (ICRA). pp. 6892–6903. IEEE (2024)
  31. Qu, D., Song, H., Chen, Q., Yao, Y., Ye, X., Ding, Y., Wang, Z., Gu, J., Zhao, B., Wang, D., et al.: Spatialvla: Exploring spatial representations for visual-language-action model. arXiv preprint arXiv:2501.15830 (2025)
  32. Shen, Y., Wei, F., Du, Z., Liang, Y., Lu, Y., Yang, J., Zheng, N., Guo, B.: Videovla: Video generators can be generalizable robot manipulators. arXiv preprint arXiv:2512.06963 (2025)
  33. Shi, L.X., Ichtter, B., Equi, M., Ke, L., Pertsch, K., Vuong, Q., Tanner, J., Walling, A., Wang, H., Fusai, N., et al.: Hi robot: Open-ended instruction following with hierarchical vision-language-action models. arXiv preprint arXiv:2502.19417 (2025)
  34. Tang, Y., Zhang, S., Hao, X., Wang, P., Wu, J., Wang, Z., Zhang, S.: Afford-grasp: In-context affordance reasoning for open-vocabulary task-oriented grasping in clutter (2025), <https://arxiv.org/abs/2503.00778>
  35. Team, G.R., Abeyruwan, S., Ainslie, J., Alayrac, J.B., Arenas, M.G., Armstrong, T., Balakrishna, A., Baruch, R., Bauza, M., Blokzijl, M., Bohez, S., Bousmalis, K., Brohan, A., Buschmann, T., Byravan, A., Cabi, S., Caluwaerts, K., Casarini, F., Chang, O., Chen, J.E., Chen, X., Chiang, H.T.L., Choromanski, K., D’Ambrosio, D., Dasari, S., Davchev, T., Devin, C., Palo, N.D., Ding, T., Dostmohamed, A., Driess, D., Du, Y., Dwibedi, D., Elabd, M., Fantacci, C., Fong, C., Frey, E., Fu, C., Giustina, M., Gopalakrishnan, K., Graesser, L., Hasenclever, L., Heess, N., Hernaez, B., Herzog, A., Hofer, R.A., Humplik, J., Iscen, A., Jacob, M.G., Jain, D., Julian, R., Kalashnikov, D., Karagozler, M.E., Karp, S., Kew, C., Kirkland, J., Kirmani, S., Kuang, Y., Lampe, T., Laurens, A., Leal, I., Lee, A.X., Lee, T.W.E., Liang, J., Lin, Y., Maddineni, S., Majumdar, A., Michael, A.H., Moreno, R., Neunert, M., Nori, F., Parada, C., Parisotto, E., Pastor, P., Pooley, A., Rao, K., Reymann, K., Sadigh, D., Saliceti, S., Sanketi, P., Sermanet, P., Shah, D., Sharma, M., Shea, K., Shu, C., Sindhvani, V., Singh, S., Soricut, R., Springenberg, J.T., Sterneck, R., Surdulescu, R., Tan, J., Tompson, J., Vanhoucke, V., Varley, J.,

- Vesom, G., Vezzani, G., Vinyals, O., Wahid, A., Welker, S., Wohllhart, P., Xia, F., Xiao, T., Xie, A., Xie, J., Xu, P., Xu, S., Xu, Y., Xu, Z., Yang, Y., Yao, R., Yaroshenko, S., Yu, W., Yuan, W., Zhang, J., Zhang, T., Zhou, A., Zhou, Y.: Gemini robotics: Bringing ai into the physical world (2025), <https://arxiv.org/abs/2503.20020>
36. Team, O.M., Ghosh, D., Walke, H., Pertsch, K., Black, K., Mees, O., Dasari, S., Hejna, J., Kreiman, T., Xu, C., et al.: Octo: An open-source generalist robot policy. arXiv preprint arXiv:2405.12213 (2024)
  37. Team, Q.: Qwen3 technical report (2025), <https://arxiv.org/abs/2505.09388>
  38. Touvron, H., Martin, L., Stone, K., Albert, P., Almahairi, A., Babaei, Y., Bashlykov, N., Batra, S., Bhargava, P., Bhosale, S., Bikel, D., Blecher, L., Ferrer, C.C., Chen, M., Cucurull, G., Esiobu, D., Fernandes, J., Fu, J., Fu, W., Fuller, B., Gao, C., Goswami, V., Goyal, N., Hartshorn, A., Hosseini, S., Hou, R., Inan, H., Kardas, M., Kerkez, V., Khabsa, M., Kloumann, I., Korenev, A., Koura, P.S., Lachaux, M.A., Lavril, T., Lee, J., Liskovich, D., Lu, Y., Mao, Y., Martinet, X., Mihaylov, T., Mishra, P., Molybog, I., Nie, Y., Poulton, A., Reizenstein, J., Rungta, R., Saladi, K., Schelten, A., Silva, R., Smith, E.M., Subramanian, R., Tan, X.E., Tang, B., Taylor, R., Williams, A., Kuan, J.X., Xu, P., Yan, Z., Zarov, I., Zhang, Y., Fan, A., Kambadur, M., Narang, S., Rodriguez, A., Stojnic, R., Edunov, S., Scialom, T.: Llama 2: Open foundation and fine-tuned chat models (2023), <https://arxiv.org/abs/2307.09288>
  39. Walke, H.R., Black, K., Zhao, T.Z., Vuong, Q., Zheng, C., Hansen-Estruch, P., He, A.W., Myers, V., Kim, M.J., Du, M., et al.: Bridgedata v2: A dataset for robot learning at scale. In: Conference on Robot Learning. pp. 1723–1736. PMLR (2023)
  40. Xi, J., He, Y., Yang, J., Dai, Y., Chai, J.: Teaching embodied reinforcement learning agents: Informativeness and diversity of language use (2024), <https://arxiv.org/abs/2410.24218>
  41. Yang, J., Tan, R., Wu, Q., Zheng, R., Peng, B., Liang, Y., Gu, Y., Cai, M., Ye, S., Jang, J., et al.: Magma: A foundation model for multimodal ai agents. In: Proceedings of the computer vision and pattern recognition conference. pp. 14203–14214 (2025)
  42. Zawalski, M., Chen, W., Pertsch, K., Mees, O., Finn, C., Levine, S.: Robotic control via embodied chain-of-thought reasoning (2025), <https://arxiv.org/abs/2407.08693>
  43. Zhang, W., Liu, H., Qi, Z., Wang, Y., Yu, X., Zhang, J., Dong, R., He, J., Lu, F., Wang, H., et al.: Dreamvla: a vision-language-action model dreamed with comprehensive world knowledge. arXiv preprint arXiv:2507.04447 (2025)
  44. Zhao, Q., Lu, Y., Kim, M.J., Fu, Z., Zhang, Z., Wu, Y., Li, Z., Ma, Q., Han, S., Finn, C., et al.: Cot-vla: Visual chain-of-thought reasoning for vision-language-action models. In: Proceedings of the Computer Vision and Pattern Recognition Conference. pp. 1702–1713 (2025)
  45. Zheng, R., Liang, Y., Huang, S., Gao, J., Daumé III, H., Kolobov, A., Huang, F., Yang, J.: Tracevla: Visual trace prompting enhances spatial-temporal awareness for generalist robotic policies. arXiv preprint arXiv:2412.10345 (2024)
  46. Zhong, Y., Huang, X., Li, R., Zhang, C., Chen, Z., Guan, T., Zeng, F., Lui, K.N., Ye, Y., Liang, Y., et al.: Dexgraspvla: A vision-language-action framework towards general dexterous grasping. arXiv preprint arXiv:2502.20900 (2025)
  47. Zhong, Z., Yan, H., Li, J., Liu, X., Gong, X., Zhang, T., Song, W., Chen, J., Zheng, X., Wang, H., et al.: Flowvla: Visual chain of thought-based motion reasoning for vision-language-action models. arXiv preprint arXiv:2508.18269 (2025)

48. Zhou, X., Xu, Y., Tie, G., Chen, Y., Zhang, G., Chu, D., Zhou, P., Sun, L.: Libero-pro: Towards robust and fair evaluation of vision-language-action models beyond memorization. arXiv preprint arXiv:2510.03827 (2025)

## Supplementary Material for “VP-VLA: Visual Prompting as an Interface for Vision-Language-Action Models”

### A Extended Ablation Results

In this section, we provide a comprehensive breakdown of our experimental evaluations to further validate the design choices of VP-VLA.

**Full Ablation Results on RoboCasa.** Table 7 presents the per-task success rates for the RoboCasa benchmark. This detailed view expands upon the main ablation study, highlighting how our design choice improves performance across diverse tabletop manipulation tasks.

**Impact of Reasoning Decomposition.** We conducted additional ablation studies in the `SimplerEnv` environment to assess the necessity of temporal decomposition. Our results in Table 8 indicate that models lacking decomposition, where both the interaction anchor (crosshair) and spatial constraint (bounding box) are rendered simultaneously, suffer a degradation in success rate, especially the “Put Eggplant in Yellow Basket” task. We hypothesize that concurrent prompts introduce visual noise that confuses the policy’s attention. Furthermore, prompting without decomposition would fail to generalize to complex, multi-step sequences, such as the “PnP \* to \* Close” task suite, where the system must distinguish between sequential objectives.

### B System 2 Planner Prompt Details

The prompt templates for the System 2 planner are provided in Table 9 and Table 10. The planner first decomposes a high-level language instruction into an ordered list of atomic subtasks. During execution, the planner is selectively invoked by transition events to re-evaluate the current stage and determine whether to proceed to the subsequent subtask. Upon triggering, the planner identifies the corresponding target object and destination names within the scene. Empirically, we find that incorporating the current gripper state into the planner’s input context enhances its decision-making accuracy regarding task completion.

### C VLA Experimental Demonstrations

To demonstrate the practical capabilities of VP-VLA, we visualize execution trajectories across simulation benchmarks and real-world deployments.

**SimplerEnv Demonstrations.** Fig. 5 illustrates the model’s performance across four distinct tasks. Given that `SimplerEnv` evaluates models in out-of-distribution (OOD) settings, success requires both high-precision localization and robust control. As shown, VP-VLA accurately decompose the manipulation process into discrete stages and effectively completes each phase.

**Table 7:** Per-task result for the ablation on Robocasa.

Task	w/o grounding	w/ all frame grounding	w/ point	w/ direct overlay	Ours (Full)
PnP Bottle To Cabinet Close	52.0	34.0	40.0	46.0	54.0
PnP Can To Drawer Close	70.0	66.0	42.0	78.0	72.0
PnP Cup To Drawer Close	48.0	54.0	32.0	48.0	44.0
PnP Milk To Microwave Close	52.0	40.0	48.0	48.0	74.0
PnP Potato To Microwave Close	42.0	46.0	30.0	26.0	34.0
PnP Wine To Cabinet Close	34.0	38.0	40.0	40.0	48.0
<b>PnP * to * Close (Avg)</b>	<b>49.7</b>	<b>46.3</b>	<b>38.7</b>	<b>47.7</b>	<b>54.3</b>
PnP Novel From Cuttingboard To Basket	50.0	60.0	58.0	52.0	66.0
PnP Novel From Cuttingboard To Cardboardbox	58.0	50.0	44.0	58.0	54.0
PnP Novel From Cuttingboard To Pan	64.0	62.0	52.0	60.0	74.0
PnP Novel From Cuttingboard To Pot	64.0	56.0	48.0	54.0	54.0
PnP Novel From Cuttingboard To Tieredbasket	36.0	40.0	42.0	46.0	56.0
<b>PnP Novel From Cuttingboard To * (Avg)</b>	<b>54.4</b>	<b>53.6</b>	<b>48.8</b>	<b>54.0</b>	<b>60.8</b>
PnP Novel From Placemat To Basket	56.0	36.0	44.0	48.0	48.0
PnP Novel From Placemat To Bowl	48.0	46.0	46.0	60.0	74.0
PnP Novel From Placemat To Plate	56.0	66.0	70.0	60.0	70.0
PnP Novel From Placemat To Tieredshelf	24.0	32.0	24.0	18.0	26.0
<b>PnP Novel From Placemat To * (Avg)</b>	<b>46.0</b>	<b>45.0</b>	<b>46.0</b>	<b>46.5</b>	<b>54.5</b>
PnP Novel From Tray To Cardboardbox	40.0	46.0	58.0	46.0	44.0
PnP Novel From Tray To Plate	52.0	56.0	56.0	66.0	66.0
PnP Novel From Tray To Pot	56.0	56.0	62.0	58.0	38.0
PnP Novel From Tray To Tieredbasket	46.0	46.0	42.0	58.0	58.0
PnP Novel From Tray To Tieredshelf	22.0	26.0	30.0	22.0	24.0
<b>PnP Novel From Tray To * (Avg)</b>	<b>43.2</b>	<b>46.0</b>	<b>49.6</b>	<b>50.0</b>	<b>46.0</b>
PnP Novel From Plate To Bowl	58.0	70.0	60.0	54.0	52.0
PnP Novel From Plate To Cardboardbox	38.0	38.0	46.0	38.0	44.0
PnP Novel From Plate To Pan	54.0	50.0	58.0	60.0	56.0
PnP Novel From Plate To Plate	66.0	74.0	62.0	74.0	62.0
<b>PnP Novel From Plate To * (Avg)</b>	<b>54.0</b>	<b>58.0</b>	<b>56.5</b>	<b>56.5</b>	<b>53.5</b>
<b>Average</b>	<b>49.4</b>	<b>49.5</b>	<b>47.3</b>	<b>50.8</b>	<b>53.8</b>

**RoboCasa Demonstrations.** Fig. 6 showcases the model’s performance on the realistic RoboCasa benchmark, which involves complex, multi-step in-

**Table 8:** Ablation result on applying task decomposition on SimplerEnv.

Method	Put Spoon on Towel	Put Carrot on Plate	Stack Green Block on Yellow	Put Eggplant in Yellow Basket	Average
Ours w/o decomposition	70.8	62.5	16.7	79.2	57.3
Ours + Qwen3VL	66.7	50.0	20.8	95.8	<b>58.3</b>

**Table 9:** Prompt structure used for task decomposition. The VLM planner decomposes a high-level task description into atomic robotic manipulation subtasks.

Section	Prompt Content
Task Description	{task_description}
Instruction	Decompose this robotic manipulation task into sequential atomic subtasks.
Subtask Types	<ul style="list-style-type: none"> <li>– Pick action (e.g., “pick up the cup”)</li> <li>– Place action (e.g., “place the cup on the table”)</li> <li>– Manipulation action (e.g., “close the drawer”, “open the microwave”)</li> </ul>
Rules	<ul style="list-style-type: none"> <li>– Keep subtask descriptions short and clear.</li> <li>– Preserve the object and location names from the original task description.</li> </ul>
Output Format	<pre>{   "subtasks": ["subtask 1", "subtask 2", ...] }</pre>

interactions in cluttered kitchen environments. These visualizations highlight VP-VLA’s ability to generalize to humanoid embodiments using egocentric observations while managing long-horizon activities.

**Real-World Demonstrations.** Fig. 7 illustrates the VP-VLA inference process in a physical environment. To achieve a successful rollout, the model must maintain precise reasoning and grounding in novel objects and unseen placement setting. The demonstration confirms that our method facilitates smooth object manipulation and placement in both in-distribution and OOD scenarios.

**Table 10:** Prompt structure used for subtask completion detection. The VLM planner determines whether the current subtask has been completed using visual evidence and gripper state information.

Section	Prompt Content
Task	{task_description}
Current Subtask	{current_subtask}
Next Subtask	{next_subtask} or "None (this is the last subtask)"
Visual Context	<ul style="list-style-type: none"> <li>– Image A: frame when the current subtask started</li> <li>– Image B: current frame</li> </ul> <p>Use visual differences between Image A and Image B to judge whether the current subtask has been completed.</p>
Gripper State	<p>LEFT_GRIPPER = {state} RIGHT_GRIPPER = {state}</p> <p>Optional notification if gripper state changes between frames: GRIPPER STATE CHANGE DETECTED: LEFT_GRIPPER: {prev_left} → {curr_left} RIGHT_GRIPPER: {prev_right} → {curr_right} This change may indicate that the current subtask has been completed.</p> <p>Consider both the visual evidence and this gripper state change when deciding whether to proceed to the next subtask.</p>
Decision Requirement	<p>Decide whether to:</p> <ul style="list-style-type: none"> <li>– CONTINUE the current subtask "{current_subtask}" (if it's still in progress)</li> <li>– PROCEED to the next subtask (if the current subtask is completed)</li> </ul> <p>Proceed only if the current subtask appears completed based on visual evidence and gripper state.</p>
Output Format Rules	<ul style="list-style-type: none"> <li>– <b>target_object</b>: noun only (e.g., bottle, drawer, cabinet)</li> <li>– <b>target_location</b>: noun phrase if applicable (e.g., cabinet shelf, counterTop surface)</li> <li>– PICK: specify only target_object</li> <li>– PLACE: specify target_object and target_location</li> <li>– OTHER actions (open/close/push): specify target_object</li> </ul>
Output Format	<pre>{   "reasoning": "...",   "decision": "continue" or "proceed",   "target_object": "&lt;noun&gt;",   "target_location": "&lt;location or null&gt;" }</pre>

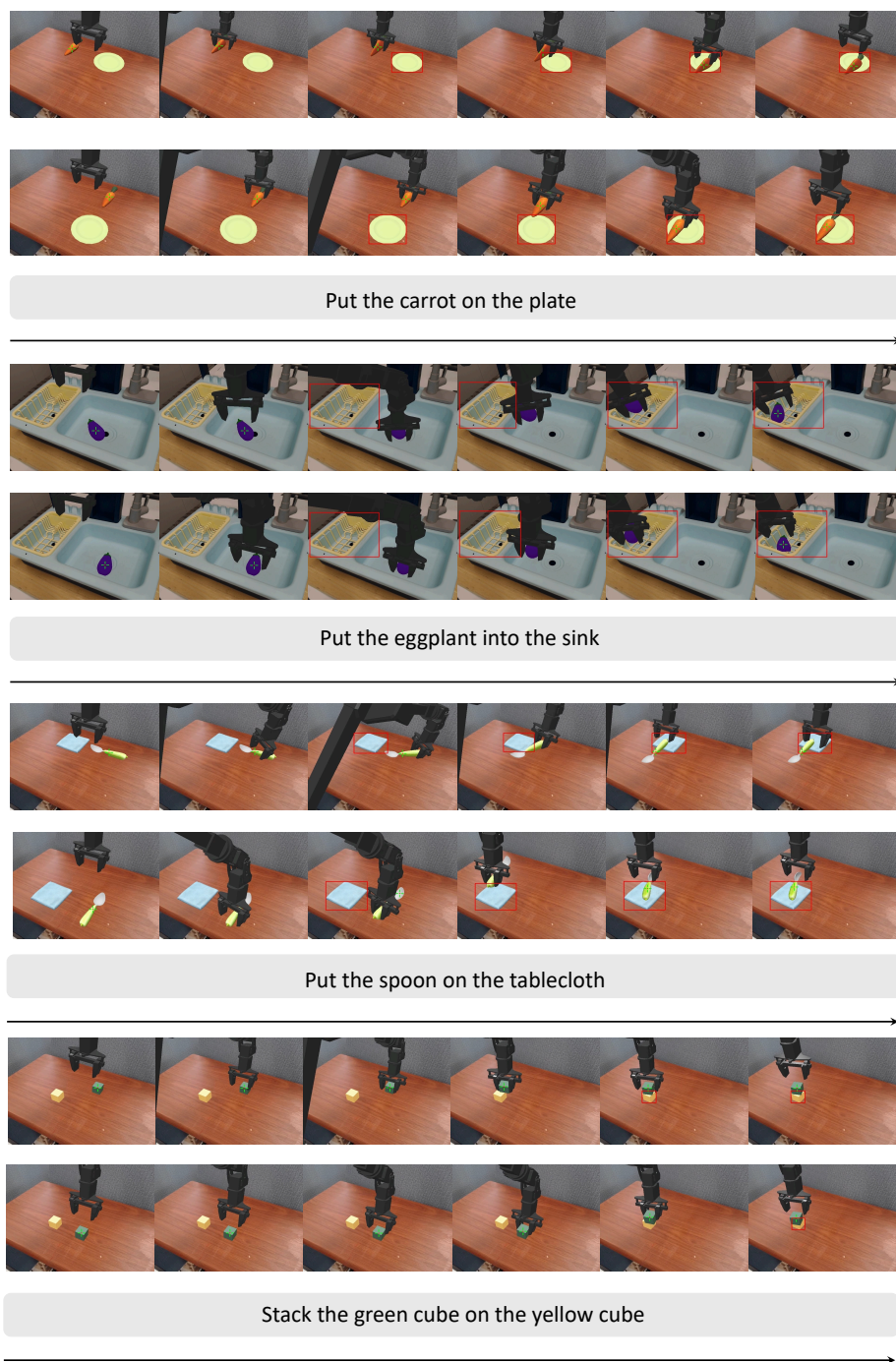
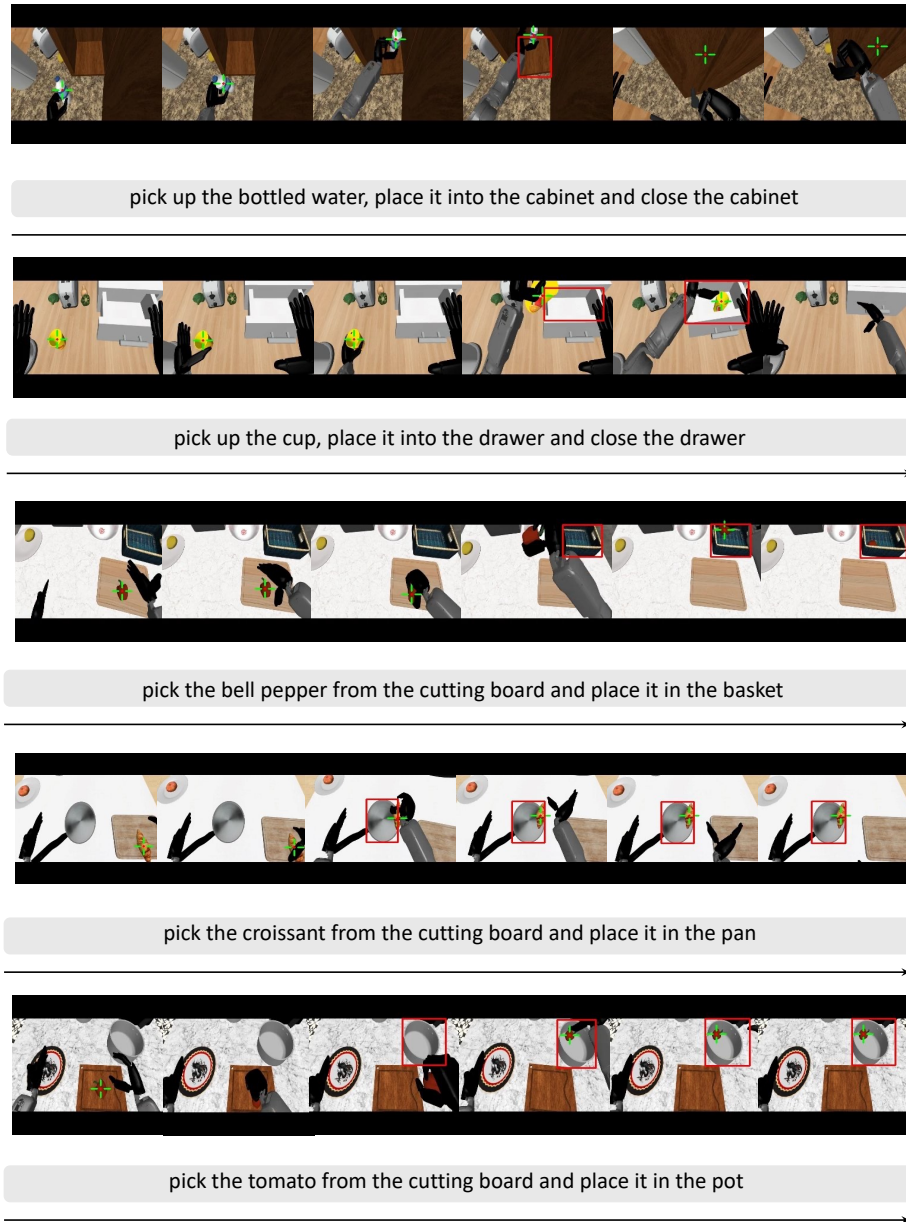
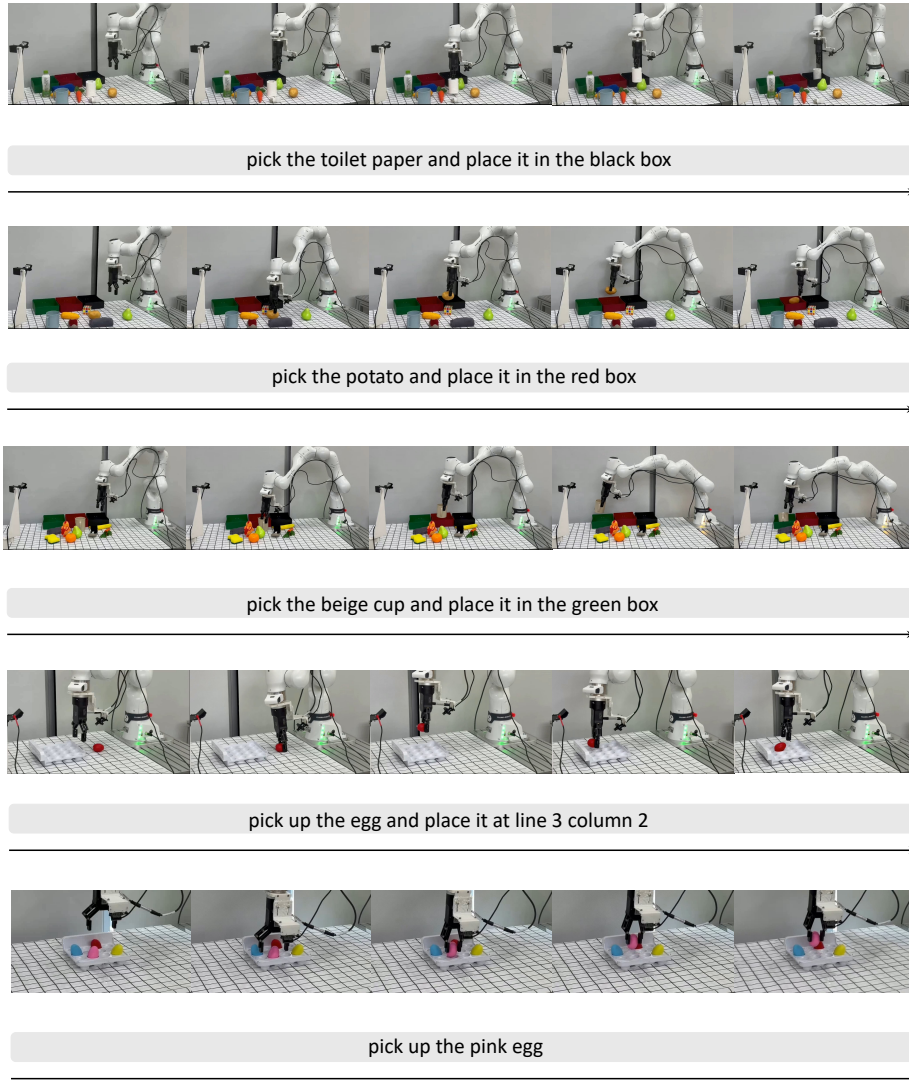


Fig. 5: Inference visualization on the SimplerEnv simulation environment.



**Fig. 6:** Inference visualization on the RoboCasa Tabletop simulation environment.



**Fig. 7:** Inference visualization on real-world tasks.